Contribution of Binary Stars to the Velocity Dispersion inside OB Associations with Gaia DR2 Data

A. M. Melnik[a,]* and A. K. Dambis[a]

[a]*Lomonosov Moscow State University, Sternberg Astronomical Institute, Moscow, Russia*
***e-mail: anna@sai.msu.ru**

Abstract—We estimated the contribution of binary systems to the velocity dispersion inside OB-associations derived from Gaia DR2 proper motions. The maximum contribution to the velocity dispersion is given by the systems with the period of revolution of $P = 5.9$ yr whose components shift by a distance of about the diameter of the system during the base-line time of Gaia DR2 observations. We employed two methods to study the motion of the photocenter of the binary system: the first one uses the total displacement between the initial and final visibility periods and the second one is based on solving a system of n equations defining the displacements at the times t_n. The first and second methods yield very similar σ_{bn} values of 0.90 and 0.87 km/s, respectively. Taking into account the fact that orbits are elliptical slightly decreases the inferred $\overline{\sigma_{bn}}$. We estimated the eccentricity-averaged $\overline{\sigma_{bn}}$ value to be $\overline{\sigma_{bn}} = 0.81$ km/s assuming that the orbital eccentricities of massive binary systems are distributed uniformly in the $e \in [0, 0.9]$ interval. The choice of the exponent γ in the power-law distribution, $p_q \sim q^{\gamma}$, of the component-mass ratios $q = M_2/M_1$ of binary systems appears to have little effect on σ_{bn}. A change of γ from 0 (flat distribution) to -2.0 (preponderance of systems with low-mass components) changes σ_{bn} from 0.90 to 1.07 km/s. The paper is based on a presentation made at the conference "Astrometry yesterday, today, tomorrow" (SAI MSU, Oct 14–16, 2019).

1. INTRODUCTION

The second intermediate data release from the satellite Gaia (Gaia DR2) contains high-precision proper motions for 1.3 billion stars derived from the position measurements collected during 1.8 year [1–3]. The average uncertainty in proper motions for high-luminosity stars of OB associations in the extended solar neighborhood is 0.1 mas/yr, which corresponds to the velocity uncertainty of 0.5 km/s at the distance of 1 kpc.

OB associations are sparse groups of stars of spectral types O and B [4]. Blaha and Humphreys [5] compiled a catalog of high luminosity stars in the extended solar neighborhood. Their list includes O−B2 type main-sequence stars, O−B3 type bright giants, and supergiants of all spectral types whose ages do not exceed 40 Myr. Blaha and Humphreys [5] identified 91 OB associations located within 3 kpc from the Sun. Of 2209 stars in OB associations 2007 (90%) were cross-matched with Gaia DR2 catalog.

A number of factors contribute to the calculated velocity dispersion inside OB associations: (1) turbulent motions inside giant molecular clouds, from which young stars form [6]; (2) motions inside binary systems, and (3) uncertainties of stellar velocities.

There is extensive evidence that giant molecular clouds are close to virial equilibrium (e.g., [7, 8]). Stars of OB associations are born in the turbulent gas medium and inherit its velocity dispersion. So the virial masses of OB associations must be nearly equal to those of their parent molecular clouds. The virial mass of an OB association can be calculated by the following formula:

$$M_{\text{vir}} = \frac{5a\sigma_t^2}{G}, \qquad (1)$$

where a is the specific radius of an association and σ_t is one-dimensional velocity dispersion of turbulent motions. The virial masses of OB associations from the catalog by Blaha and Humphreys [5] lie in the interval 10^5–10^7 $M_\odot$ [9, 10], which, on the whole, is consistent with the mass estimates of giant molecular clouds: 10^5–2×10^6 $M_\odot$ [11].

We use Gaia DR2 proper motions to calculate the velocity dispersions inside OB associations in the direction of the Galactic longitude l and latitude b. We then corrected the observed velocity dispersions, $\sigma_{l,\text{obs}}$

and $\sigma_{b,\text{obs}}$, for the errors in proper motions and distances:

$$
\begin{aligned}
\sigma_{vl}^2 &= \sigma_{l,\text{obs}}^2 - (4.74 r \varepsilon_{\mu l})^2 - (4.74 a \overline{\mu_l})^2, \\
\sigma_{vb}^2 &= \sigma_{b,\text{obs}}^2 - (4.74 r \varepsilon_{\mu b})^2 - (4.74 a \overline{\mu_b})^2,
\end{aligned}
\tag{2}
$$

where $\varepsilon_{\mu l}$ and $\varepsilon_{\mu b}$ are the average uncertainties in Gaia DR2 proper motions; $\overline{\mu_l}$ and $\overline{\mu_b}$ are average proper motions of stars in an association in the direction of the Galactic longitude and latitude, respectively; r is the heliocentric distance of the OB association; the factor $4.74 r$ [kpc] transforms units of mas/yr into km/s. In our calculations of the sky-plane velocities we use the average distance r to the association and do not use parallaxes of individual stars. In this case the average error in distances is about the specific radius a of the association in the sky plane. The average dispersion caused by the errors in Gaia DR2 proper motions is 0.5 km/s. The errors in distances to individual stars (the last term in Eq. (2)) also create an additional velocity dispersion with the average value equal to 0.5 km/s.

The average one-dimensional velocity dispersion calculated for 28 OB associations including more than 20 stars with known Gaia DR2 proper motions is $\sigma_v = 4.5$ km/s. The velocity dispersion inside OB associations has not been corrected for binary-star effect which was taken, by default, to be small [10].

However, the fraction of binary systems among OB stars is quite large and amounts to 30−100% [12−15]. In this paper we estimate the contribution of binary systems to the velocity dispersion inside OB associations by simulating the motion of binary components.

2. RESULTS

2.1. Shift of the Photocenter of the Binary System between the First and Final Gaia DR2 Visibility Periods

The shift of the component of the binary system during the Gaia DR2 base-line time ($T = 1.8$ year) gives rise to additional proper motion and hence additional velocity which increases the velocity dispersion inside OB associations.

Let us consider a binary system with the components moving in circular orbits in the sky plane with the revolution period of P (Fig. 1a). The primary and secondary components are named as 1 and 2, respectively. A typical representative of an OB association member star in the catalog by Blaha and Humphreys [5] is a 10 $M_\odot$ star, and we therefore assume that the mass of the primary is $M_1 = 10 M_\odot$ and that of the secondary component is $M_2 = q M_1$:

$$
q = M_2 / M_1 < 1. \tag{3}
$$

The binary components are rotating around the mass centre O in orbits with the radii a_1 and a_2, respectively.

The radius a_2 can be estimated from Newton's gravity law:

$$
a_2^3 = \frac{P^2}{4\pi^2} \frac{G M_1}{(1+q)^2}, \tag{4}
$$

and the radius a_1 can be derived from the relation:

$$
a_1 = q a_2. \tag{5}
$$

The displacements s_1 and s_2 of binary components between the first and final visibility periods of Gaia DR2 measurements are equal to:

$$
S_2 = \sqrt{2} a_2 \sqrt{1 - \cos \frac{2\pi T}{P}}, \tag{6}
$$

$$
S_1 = q S_2, \tag{7}
$$

where T is the base-line time of Gaia DR2 observations.

However, Gaia DR2 observations include many visibility periods of individual stars. For example, stars of OB associations were observed, on average, during $n = 14$ visibility periods. The number of visibility periods is the number of groups of observations separated from other groups by at least 4 days [3, 16]. In Section 2.2 we consider another method based on solving a system of n equations defining the displacements s_n at the times t_n.

Binary systems with the period of $P = 5.9$ yr appear to give the maximal contribution to the velocity dispersion. In this case the displacement $S = S_1 + S_2$ of the components between the initial and final visibility periods of Gaia DR2 observations is nearly equal to the diameter of the orbit $D \approx a_1 + a_2$ and amounts to $D \approx 8$ a. u., which corresponds to the angular separation between the components of ~8 mas at the distance of $r = 1$ kpc. Note that the median heliocentric distance of OB associations in the catalog by Blaha and Humphreys [5] is $r = 1.7$, i.e., the median angle between the binary components must be 1.7 times smaller.

Stellar images in the Gaia focal plane have large sizes and this is done intentionally to increase the number of pixels involved in image building and allow the position of the image center to be determined with greater accuracy. The median size of Gaia images (the full width at half maximum of the line spread function) is ~ 100 mas [17]. It means that the binary stars considered must be represented by the same source.

Thus, we should consider the displacement of the photocentre of the binary system but not the motion of one of its components. Generally, calculating the effect of binaries requires a consideration of Gaia's line spread function, point spread function and source detection algorithm. Here we do not claim to derive the full solution but at the first approximation, we can
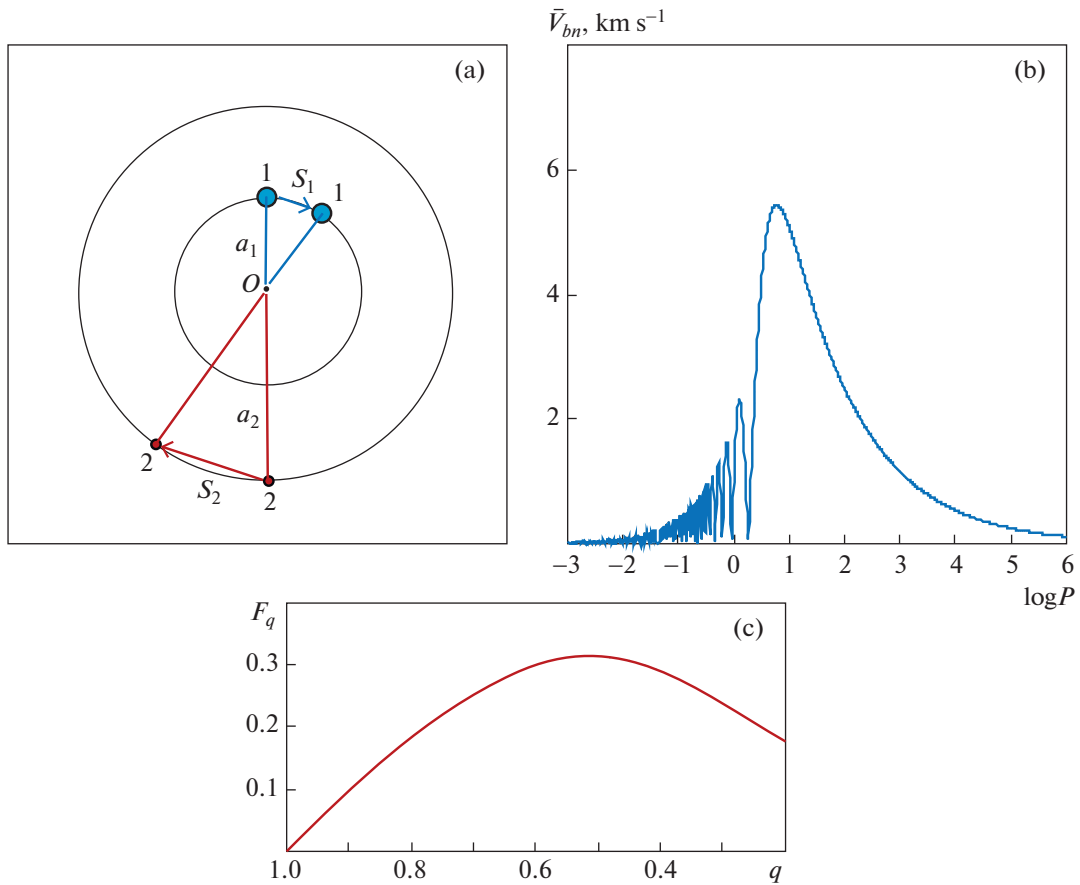
Fig. 1. Contribution of binary systems to the velocity dispersion inside OB-associations. (a) Model of a binary system with component stars named 1 and 2 rotating around the common mass center in circular orbits in the sky plane with the period of revolution P. The vectors S_1 and S_2 indicate the displacements of binary stars over the base-line time of Gaia DR2 measurements, T. The mass centre is located at point O. The radii of orbits of components 1 and 2 are a_1 and a_2, respectively. (b) Dependence of the additional velocity $\overline{V_{bn}}$ averaged over mass ratio q on $\log P$. The velocity $\overline{V_{bn}}$ is the average contribution of a binary system with a period P into the velocity dispersion. The maximal value of the velocity $\overline{V_{bn}}$ is 5.4 km/s corresponding to the period $P = 5.9$ yr. (c) Dependence of function F_q (Eq. (11)) on mass ratio q. Function F_q equals zero at $q = 1$ implying the fixed position of the photocentre of a binary system with equal-mass components, and reaches maximum at $q = 0.52$.

suppose that the line spread and point spread functions are nearly flat within ±10 mas from the maximum [17].

We can further assume that the light flux from both binary components determines the position of the centre of the image. We then use the following relation between the luminosity L of a star and its mass M, for example [18]:

$$L \sim M^4, \qquad (8)$$

to write the following formula for the displacement of the photocentre of the binary system:

$$S_{\mathrm{ph}} = \frac{S_1 M_1^4 - S_2 M_2^4}{M_1^4 + M_2^4}. \qquad (9)$$

Substituting the variables from Eqs (4)−(7) we have

$$S_{\mathrm{ph}} = \sqrt{2}\left(\frac{GM_1 P^2}{4\pi^2}\right)^{1/3}\sqrt{1 - \cos\frac{2\pi T}{P}}F_q, \qquad (10)$$

where function F_q is equal to

$$F_q = \frac{q - q^4}{(1 + q^4)(1 + q)^{2/3}}. \qquad (11)$$

Figure 1c shows the variation of function F_q which equals zero at $q = 1$. The motion of two identical sources in the sky plane indeed does not produce a shift of their common photocentre. On the other hand, if one of the components is too small then the displacements of the primary component would be negligible. Function F_q reaches maximum at $q = 0.52$.

The motion of the photocentre of the binary system creates the additional velocity, which affects the observed stellar velocity in the sky plane:

$$V_{bn} = S_{ph}/T, \quad (12)$$

where T is time base-line of Gaia DR2 observations. Figure 1b shows the dependence of the additional velocity $\overline{V_{bn}}$ averaged over mass ratio, q, on $\log P$. On the whole, the dependence of $\overline{V_{bn}}$ on the period P can be easily understood: at small periods the binary systems have small diameters and the displacements of the photocenter are small, the larger P the larger the diameter D of the system, but in this case the orbital velocities are low and the displacements of the photocenter during the Gaia DR2 base-line time are small. Consequently, there is a certain period P corresponding to the maximal shift S_{ph}. The maximal shift S_{ph} and consequently the maximal velocity $\overline{V_{bn}}$ are achieved for $P = 5.9$ yr. The maximal velocity is equal to 5.4 km/s. At small periods the velocity $\overline{V_{bn}}$ demonstrates oscillations and zero values $\overline{V_{bn}} = 0$ correspond to the periods $P = T/n$, where n is integer and the binary system makes a whole number of revolutions within time interval T, resulting in zero displacement S_{ph}.

To estimate the effective contribution of binary stars, σ_{bn}, to the velocity dispersion inside an OB association, σ_v, we integrate $V_{bn}^2(P,q)$ over all possible periods and mass ratios:

$$\sigma_{bn}^2 = f_b f_j \int_{q=0.2}^{q=1.0} \int_{\log P=-3}^{\log P=+6} V_b^2(P,q) f_p(P) p(q) d(\log P) dq, \quad (13)$$

where factors f_b and f_j characterize the fraction of binary stars and projection effects, while functions $f_p(\log P)$ and $f_q(q)$ take into account the period and mass-ratio distributions, respectively. Here we make the following assumptions. The fraction of binary systems in OB associations amounts to $f_b = 0.5$ [13]. The ensemble of binary systems is thought to be oriented randomly with respect to the line of sight and consequently the squared projection of the total velocity V into a random direction, for example, x, amounts, on average, to $V_x^2 = 1/3 V^2$, which gives a projection factor of $f_j = 1/3$. Aldoretta et al. [19] showed that the period distribution of massive binary stars is approximately flat in increments of $\log P$ (so-called Öpik's law [20, 21]) in the interval of $\log P$ from -3 to $+6$. So we can suppose that $f_p = 1/9$ for unit of $\log P$. Sana and Evans [22] found that the distribution of binary systems over mass ratio q is uniform within the interval $q = 0.2$–1.0 so we can adopt $f_q = 1.25$.

We now integrate Eq. (13) numerically to determine the average contribution of binary systems to the velocity dispersion inside OB associations:

$$\sigma_{bn} = 0.90(M_1/10\,M_\odot)^{1/3}, \quad (14)$$

which is more than twice greater than $\sigma_{bn} = 0.38$ km/s derived for the time base-line of Gaia DR1 observations equal to T [23]. Both these values of σ_{bn} are rather small compared to the observed velocity dispersion, $\sigma_v = 4$–5 km/s. Eq. (14) shows that σ_{bn} depends only slightly on mass M_1: a 10 times decrease of the mass (from $M_1 = 10$ to 1 $M_\odot$) translates in only a ~2 times decrease in σ_{bn}.

2.2. Shift of the Photocenter of the Binary System Estimated Taking into Account Intermediate Gaia DR2 Observations

Let us assume that the position of the photocenter of the binary system is measured n times during Gaia DR2 base-line time. For definiteness, we adopted $n = 14$, which corresponds to the average number of Gaia DR2 visibility periods for high-luminosity stars from the catalog by Blaha and Humphreys [5]. Figure 2a shows the rotation of components of the binary system with the period of revolution equal to $P = 5.9$ yr providing the maximal displacement of the protocenter during Gaia DR2 base-line time. Figure 2b shows the rotation of the photocenter C around the mass center O of the system. The radius of the orbit of the photocenter equals:

$$a_{ph} = \left(\frac{GM_1 P^2}{4\pi^2}\right)^{1/3} F_q. \quad (15)$$

The vector $\vec{S}$ is the displacement between the initial and final visibility periods. Let us set the coordinate system with the x axis parallel to the vector $\vec{S}$ and the y axis perpendicular to it. The chord c_n shows the shift of the protocenter by the time t_n. Projections of the chord c_n onto the directions x and y are equal to x_n and y_n, respectively. The maximal shift of the photocenter occurs along the x axis, but in the perpendicular direction the protocenter deviates by a distance of $\sim|\vec{S}|/2$ and returns to close to the initial position. The additional velocities V_x and V_y in the directions x and y can be derived by solving the following systems of equations:

$$\begin{aligned} x_n &= x_0 + V_x t_n, \\ y_n &= y_0 + V_y t_n. \end{aligned} \quad (16)$$

respectively. Since we calculate one-dimensional velocity dispersion σ_{bn} and take projection effect into
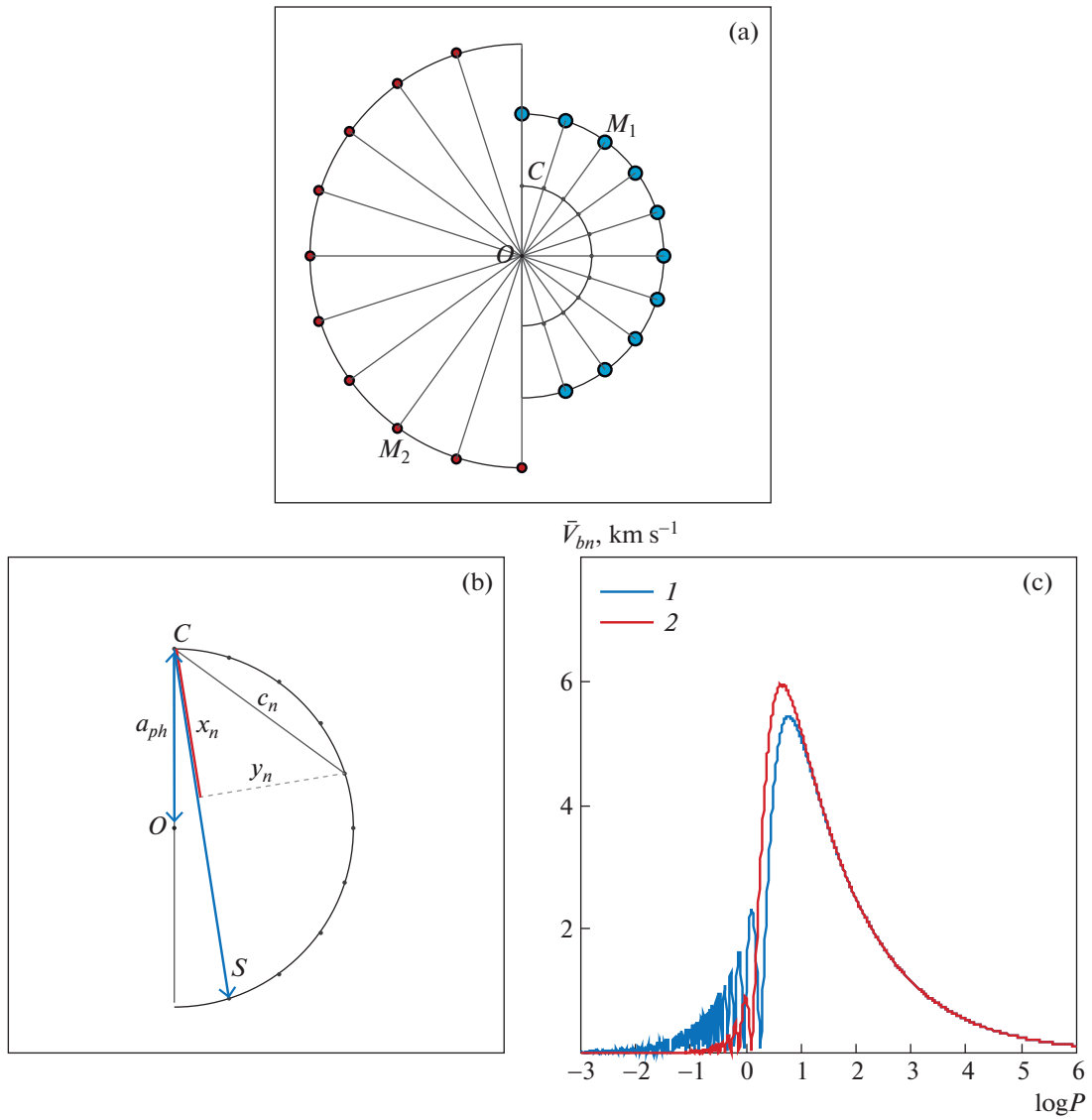
Fig. 2. (a) Binary system with the components M_1 and M_2 rotating around their common mass center O. The position of the photocenter at the initial moment is indicated by the point C. (b) The motion of the photocenter C along the circle of radius a_{ph}. The position of the photocenter is measured n times during the Gaia DR2 base-line time. The vector S connects the positions of the photocenter between the initial and final visibility periods. The chord c_n shows the displacement of the photocenter by the time t_n while x_n and y_n are its projections onto the direction S and onto the perpendicular direction, respectively. (c) The dependence of the additional velocity $\overline{V_{bn}}$ averaged over q on $\log P$ derived by two methods: one using the total displacement S between the initial and final visibility periods (the blue line) and another based on solving a system of n equations defining the displacements x_n at the times t_n (the red line). The maximal velocities $\overline{V_{bn}}$ calculated by the first and second methods are 5.4 and 6.0 km/s, respectively.

account through the factor $f_j = 1/3$, we have to find the maximal possible displacement in one direction. It means that:

$$V_{bn} = V_x. \qquad (17)$$

Note that the velocity V_y and the additional proper motion (Eq. (32)) are calculated with a large error, which could lead to the large size of error ellipsoid in

determination of 5 astrometric parameters (α, δ, μ_α, μ_δ and ϖ) of a star and causes their subsequent rejection [3]. This problem will be discussed in section 2.5.

Figure 2c shows the dependence of the additional velocity $\overline{V_{bn}}$ averaged over q on $\log P$ based on two methods: one using the total displacement S between the initial and final visibility periods (section 2.1) and another based on solving a system of n equations
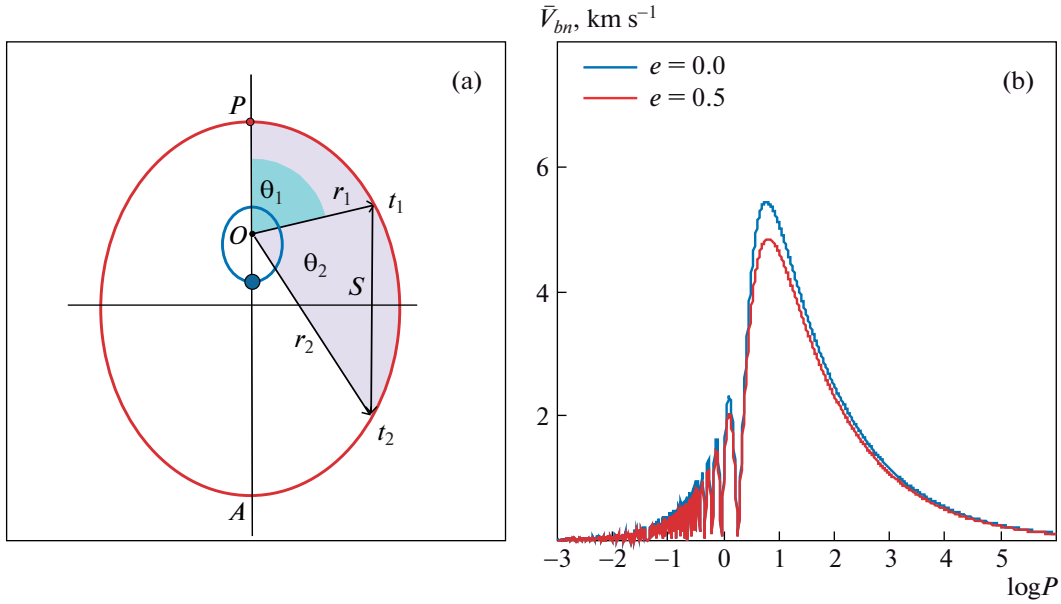
Fig. 3. (a) Elliptical orbits of components 1 and 2 of the binary system are shown as the small and large ellipses, respectively. The foci of the orbits and the system mass center are located at the point O. The points P and A indicate the positions of the pericenter and apocenter of the orbit of the secondary component. The angles θ_1 and θ_2 are counted from the pericenter P and correspond to the positions of the secondary component at the initial t_1 and final t_2 visibility periods of Gaia DR2 observations, respectively. (b) Dependence of the additional velocity $\overline{V_{bn}}$ averaged over the parameters q and t_1 ($t_1 \in [0, P]$) on $\log P$ calculated for orbits with the eccentricity $e = 0.5$ (the red line) and $e = 0$ (the blue line).

defining the displacements x_n at the times t_n. The maximal velocities $\overline{V_{bn}}$ calculated by the first and second methods are 5.4 and 6.0 km/s, respectively. The maximal velocity $\overline{V_{bn}}$ calculated by the second method has a larger value ($\overline{V_{bn}} = 6$ km/s), but at small periods, where the oscillations occur, $\overline{V_{bn}}$ takes smaller values than the velocity calculated by the first method.

We integrate the velocity $\overline{V_{bn}}$ over the increment $\log P$ to obtain the average contribution of binary systems to the velocity dispersion computed taking into account intermediate measurements:

$$\sigma_{bn} = 0.87(M_1/10\,M_\odot)^{1/3}. \tag{18}$$

Thus, the average contributions of binary systems to the velocity dispersion inside OB associations calculated by the two methods differ only by 3%.

2.3. Elliptical Orbits

The distribution of massive binary systems over the eccentricity e depends on the period: long-period systems ($P > 10$ yr) have practically uniform distribution over the eccentricity while short-period systems ($P < 100$ days) demonstrate the excess of circular orbits [13, 15, 24, 25].

Let us consider a binary system with the eccentricity of $e = 0.5$ and estimate the contribution of these systems into the velocity dispersion inside OB associations. Figure 3a shows the binary system with the components moving in elliptical orbits whose foci are located at the mass center O. The points P and A indicate the positions of the pericenter and apocenter, respectively, of the orbit of the secondary component; the angles θ_1 and θ_2 are counted from the pericenter P and correspond to the positions of the secondary component at the initial t_1 and final t_2 visibility periods of Gaia DR2 observations, respectively.

The motion of material body in an elliptical orbit is defined by Kepler's law:

$$E - \sin E = M, \tag{19}$$

where E is eccentric anomaly and M is mean anomaly:

$$M = \frac{2\pi}{P}(t - t_0), \tag{20}$$

where t_0 is the pericenter passage time. If we know the eccentric anomaly E we can calculate the true anomaly, the angle θ between the direction to the secondary

component at the moment t and the direction to the pericenter [26]:

$$\sin\theta = \frac{\sqrt{1-e^2}\sin E}{1-e\cos E},$$
$$\cos\theta = \frac{\cos E - e}{1 - e\cos E}. \qquad (21)$$

The distance r from the mass center to the secondary component at the time t is determined by the relation:

$$r = \frac{a\sqrt{1-e^2}}{1+e\cos\theta}, \qquad (22)$$

where a is the semi-major axis of the secondary-component orbit, which depends on the period of the binary, P, the mass of the primary component, M_1, and the mass ratio, q (Eq. (4)).

We calculate the eccentric anomaly E to an accuracy of the order of 10^{-6} radian using the iterative method proposed by Danby [27]. In zero approximation $E_0 = M + 0.85e$ and each subsequent value is determined by:

$$E_{n+1} = E_n$$
$$-\frac{(M+e\sin E_n - E_n)^2}{E_n - 2(M+e\sin E_n) + M + e\sin(M + e\sin E_n)}. \qquad (23)$$

The time $t_1 \in [0, P]$ determines the angle θ_1 and the radius r_1 at the initial visibility period of Gaia DR2. The time t_2 corresponds to the final visibility period of Gaia DR2:

$$t_2 = t_1 + T. \qquad (24)$$

For each time t_1, we calculated the time t_2, the angles θ_1 and θ_2, the distances r_1 and r_2, as well as the displacement of the secondary component:

$$S_2 = \sqrt{r_1^2 + r_2^2 - 2r_1 r_2 \cos(\theta_2 - \theta_1)}. \qquad (25)$$

The displacement of the primary component S_1 is determined by Eq. (7). With the knowledge of S_1 and S_2 we can find the shift of the photocenter S_{ph} (Eq. (10)) and additional velocity V_{bn} (Eq. (12)).

Figure 3b shows the dependence of the additional velocity $\overline{V_{bn}}$ averaged over the parameters q and t_1 ($t_1 \in [0, P]$) on $\log P$ calculated for orbits with the eccentricity $e = 0.5$. In that case the maximal velocity amounts to $\overline{V_{bn}} = 4.8$ km/s. For comparison, we also present the velocity $\overline{V_{bn}}$ obtained for circular orbits by the method outlined in section 2.1. As is evident from the figure, the assumption of the orbit ellipticity slightly decreases the additional velocity $\overline{V_{bn}}$.

The average contribution of elliptical orbits with $e = 0.5$ to the velocity dispersion inside OB associations is:

$$\sigma_{bn} = 0.82(M_b/10\,M_\odot)^{1/3}, \qquad (26)$$

which is ~10% less than the value of 0.90 km/s obtained for circular orbits (Eq. (14)). This is probably due to the fact that the secondary component spends most of its time near the apocenter of the orbit where it rotates with a low angular velocity shifting by a small angle during the Gaia DR2 base-line time, and its large distance r from the mass center cannot compensate the low angular velocity.

It turned that the change of the eccentricity of orbits of binary systems from $e = 0$ to 0.9 results in a change in σ_{bn} from $\sigma_{bn} = 0.90$ to 0.58 km/s. Assuming that the orbital eccentricities e of massive binary systems are distributed uniformly over the interval $e \in [0, 0.9]$, we calculated the value of $\overline{\sigma_{bn}}$ averaged over eccentricity:

$$\overline{\sigma_{bn}} = 0.81(M_b/10\,M_\odot)^{1/3}, \qquad (27)$$

which practically coincides with the result obtained for the eccentricity of $e = 0.5$.

2.4. Another Distribution of p_q

In previous sections we suppose that the mass ratios $q = M_2/M_1$ of massive binary systems are distributed uniformly over the interval $q \in [0.2, 1]$ [20]. However, there is an opinion that the distribution of the mass ratios of binary stars p_q is shifted towards small q and can be described by a power law $p_q \sim q^\gamma$, where γ lies in the range from -0.5 to -2.4 [15].

Figure 4 shows the probability distribution $p_q = Cq^\gamma$ obtained for $\gamma = 0$ (constant distribution), $\gamma = -0.5$, -1.0, -1.5, and -2.0. The constant C is derived from the normalization condition:

$$\int_{q=0.2}^{q=1.0} p_q = 1. \qquad (28)$$

Integrating V_{bn}^2 (Eq. (13)) with the function $p_q = Cq^\gamma$ for exponent $\gamma = -1.5$ yields the following velocity dispersion σ_{bn}:

$$\overline{\sigma_{bn}} = 1.07(M_b/10\,M_\odot)^{1/3}, \qquad (29)$$

which is greater than $\sigma_{bn} = 0.90$ km/s calculated for the flat distribution p_q by only 18%. On the whole, the choice of exponent γ has little effect on the inferred σ_{bn}: a change of γ from 0 to -2.0 results in a variation σ_{bn} in the range from 0.90 to 1.07. This is due to the fact that the maximal contribution to the velocity dispersion is given by systems with the component mass
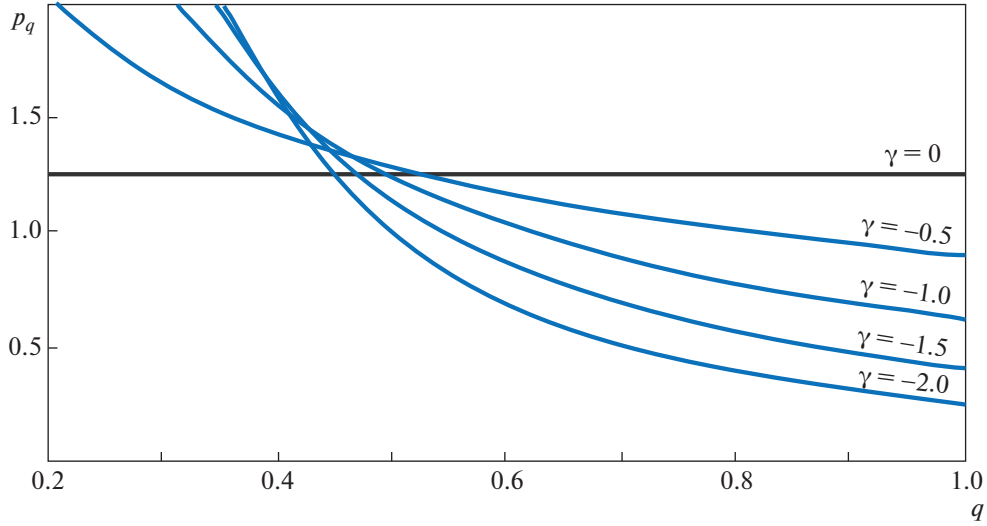
Fig. 4. Distribution of component mass ratios q of binary systems: $p_q = Cq^\gamma$, for $\gamma = 0$ (flat distribution), $\gamma = -0.5$, -1.0, -1.5, and -2.0.

ratio $q = 0.5$ at which all functions p_q considered have close values (Fig. 4).

2.5. Analysis of Errors in Proper Motions Caused by Motions of the Photocenter of Binary System

The maximum contribution to the velocity dispersion derived from Gaia DR2 data is provided by binary systems with the period of $P = 5.9$ yr. However, the photocenter moves practically linearly in one direction and makes a swing in the other direction, which has nothing in common with linear motion. In this section we analyze errors in proper motions due to nonlinear motions.

Figure 5 shows the positions of the photocenter of a binary system at different times, and the proper motions derived from these positions. The times are chosen randomly within the base-line time interval of Gaia DR2. The x axis coincides with the vector $\vec{S}$ connecting the positions of the photocenter between the initial and final visibility periods and the y axis is perpendicular to the x one (Fig. 2b). We take as an example a binary system with the period $P = 5.9$ yr, which gives the maximal contribution to the shift of the photocenter. For convenience of the transformation into angular units, we place the binary system at a heliocentric distance of $r = 1$ kpc. The proper motions of the photocenter, μ_x and μ_y, are derived by solving the system of linear equations defining the sky positions of the photocenter (x'_n, y'_n) at different times. 0

$$x'_n = x'_0 + \mu_x t_n,$$
$$y'_n = y'_0 + \mu_y t_n, \tag{30}$$

where x'_n, x'_0, y'_n and y'_0 are in the units of mas and the proper motions, μ_x and μ_y, are in the units of mas/yr:

$$x'_n = 2.06265 \times 10^8 x_n/r,$$
$$x'_0 = 2.06265 \times 10^8 x_0/r,$$
$$y'_n = 2.06265 \times 10^8 y_n/r, \tag{31}$$
$$y'_0 = 2.06265 \times 10^8 y_0/r,$$

$$\mu_x = V_x/(4.74r),$$
$$\mu_y = V_y/(4.74r). \tag{32}$$

Figures 5a, 5b show that the displacement of the photocenter along the x axis obeys a linear law while the displacement along the y axis outlines an arc, significantly increasing the errors in determination of the coordinate y_0 and proper motion μ_y. On the whole, the motion along an arc implies at least quadratic dependence on time.

We also consider the influence of the parallactic displacement on the derived values of proper motions. Figures 5c,d show the motion of the photocenter of the binary system distorted by the parallactic displacement. For convenience, the amplitudes of parallactic motions along the x and y axes were adopted to be $P_x = P_y = 1$ mas.

$$p_x = P_x \cos(2\pi t_n + \varphi_0),$$
$$p_y = P_y \sin(2\pi t_n + \varphi_0). \tag{33}$$

We can see that the slopes of straight lines in Figs. 5a, 5c as well as in Figs. 5b, 5d are almost the same, indicating that the parallactic displacement has only a minor effect on the derived values of proper motions.
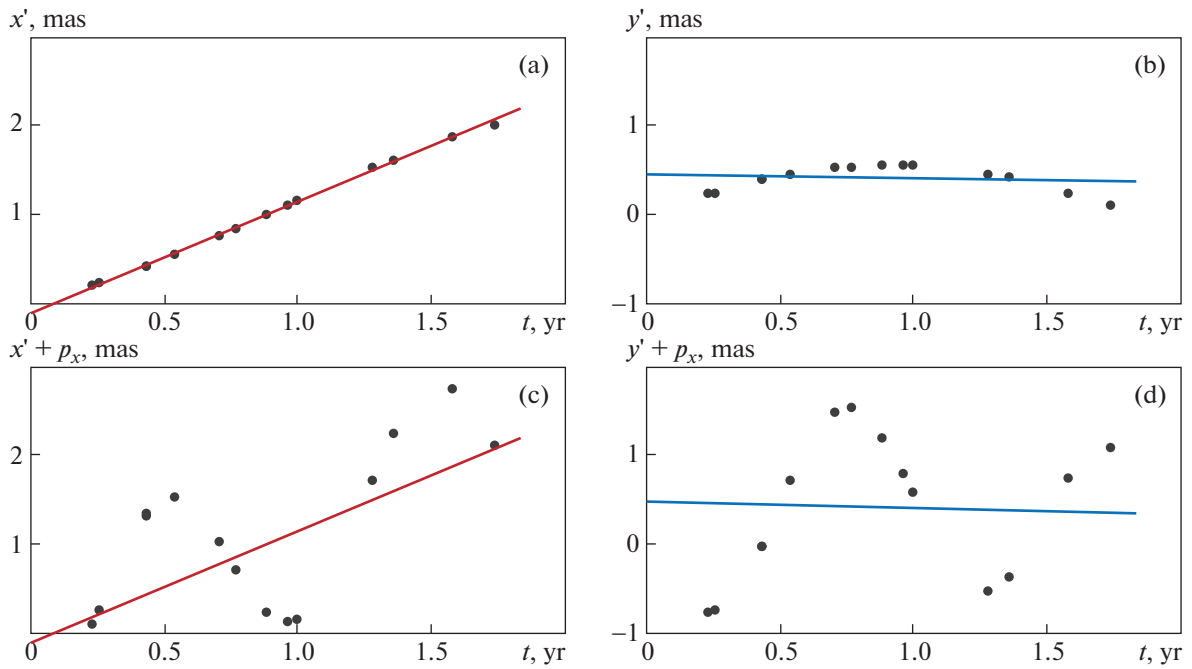
Fig. 5. Positions of the photocenter of the binary system at different time instants (points) and the proper motions derived from them (straight lines). The x axis coincides with the vector S connecting the positions of the photocenter between the initial and final visibility periods and the y axis is perpendicular to the x axis (Fig. 2b). As an example we chose a binary system with the period $P = 5.9$ yr providing the maximal contribution to the shift of the photocenter. For convenience of the transformation into angular values, the binary system was placed at the distance of $r = 1$ kpc from the Sun. (a, b) Positions of the photocenter obtained without taking into account the parallactic displacement. (c, d) positions with the parallactic displacement taken into account. We can see that the slopes of the straight lines in panels (a and c) as well as in panels (b and d) are almost the same and this fact indicates that the parallactic displacement has only a slight effect on the derived proper motions. The displacement of the photocenter along the x axis (a) obeys a linear law while the displacement along y axis (b) outlines an arc, resulting in a significant increase of the errors in the determination of the coordinate y_0 and proper motion μ_y.

Table 1 lists proper motions, μ_x and μ_y, and their errors as well as the errors of the coordinates x_0 and y_0 (the coordinates themselves are not of interest in our case) calculated for the motion of the photocenter of the binary system with and without taking into account the parallactic displacement. We can see that the accuracy of the determination of the coordinate and proper motion along the x axis is almost one order of magnitude higher than along the y axis. For example, the errors in the determination of x_0 and μ_x are 0.01 mas and 0.01 mas/yr, respectively, but the errors in y_0 and μ_y amount to 0.1 mas and 0.1 mas/yr, respectively.

Thus, the motion of the photocenter of the binary system practically does not increase the uncertainty in the determination of the proper motion in one direction and adds an extra uncertainty of 0.1 mas/yr in the determination of the proper motion in the other direction. The average uncertainty of proper motions of stars of OB associations is 0.1 mas/yr so the binary system considered will have the uncertainties in the proper motions in the range 0.1−0.2 mas/yr.

Lindegren et al. [3] formulated three conditions under which a five parameter solution derived from Gaia DR2 measurements would not be rejected: 4

$$
\begin{aligned}
&(1) \quad \text{mean magnitude } G \leq 21.0^{m}, \\
&(2) \quad \text{visibility periods used} \geq 6, \\
&(3) \quad \text{astrometric sigma5d} \\
&\qquad \text{max} \leq (1.2'' \text{ mas}) \times \gamma(G),
\end{aligned}
\quad (34)
$$

where $\gamma(G) = \max[1, 10^{0.2(G-18)}]$.

Table 1. Errors in coordinates and proper motions

	$\pm\varepsilon_{x0}$, mas	$\pm\varepsilon_{y0}$, mas	$\mu_x \pm \varepsilon_{\mu x}$, mas/yr	$\mu_y \pm \varepsilon_{\mu y}$, mas/yr
$P_x = P_y = 0$	± 0.012	± 0.085	1.248 ± 0.012	-0.046 ± 0.086
$P_x = P_y = 1$ mas	± 0.012	± 0.085	1.260 ± 0.009	-0.077 ± 0.090

The average G-band magnitude and the average number of visibility periods for member stars of OB associations are $\overline{G} = 8.5^m$ and $n_{vis} = 14$, respectively. Hence the first two conditions are easily satisfied. The third condition is that a five-dimensional equivalent to the semi-major axis of the position error ellipse, astrometric_sigma5d_max, must not exceed 1.2 mas [3]. The nonlinear motions of the photocenter of the binary system considered produce the errors at the level of 0.1 mas, which is nearly an order of magnitude less than the threshold value of 1.2 mas (Eq. (34)). Thus, the calculated five-parameter solution for the motion of the photocenter of the binary system will not be rejected.

Note that the binary systems of other periods produce smaller displacements of the photocenter and, consequently, the errors due to nonlinear motions must be smaller as well.

Furthermore, the median heliocentric distance of OB associations in the catalog by Blaha and Humphreys [5] is $r = 1.7$ kpc and, consequently, the median errors of the proper motions must be 1.7 times smaller.

3. CONCLUSIONS

We estimated the contribution of binary systems to the velocity dispersion inside OB associations derived from Gaia DR2 proper motions. Its average value is $\sigma_{bn} = 0.90$ km/s. The maximum contribution to the velocity dispersion is provided by the systems with the period of revolution of $P = 5.9$ yr whose components shift at the distance close to the diameter of the system during the base-line time of Gaia DR2 observations. These systems have a diameter of ~8 a. u., which corresponds to the angular separation of ~8 mas at the distance of 1 kpc from the Sun. The characteristic size of images in the focal plane of Gaia satellite is ~100 mas, implying that both components of the binary system form a single image.

We studied the motion of the photocenter of the binary system by two methods: one using the total displacement S between the initial and final visibility periods and another based on solving a system of n equations defining the displacements x_n at the times t_n. As stars of OB associations [5] were observed, on average, during 14 visibility periods, we adopted $n = 14$. The first and second methods yield very similar values of 0.90 and 0.87 km/s.

We analyzed the effect of ellipticity of orbits of binary stars on the estimated velocity dispersion inside OB associations σ_{bn}. It turns that accounting for the orbit eccentricity decreases σ_{bn} by 10%. For example, orbits with the eccentricity of $e = 0.5$ yield $\sigma_{bn} = 0.82$ km/s. Assuming that the orbital eccentricities of massive binary systems are distributed uniformly over the

interval $e \in [0, 0.9]$, we obtained the eccentricity-averaged $\overline{\sigma_{bn}}$ to be $\overline{\sigma_{bn}} = 0.81$ km/s.

The choice of exponent γ in the power distribution $p_q \sim q^\gamma$, where $q = M_2/M_1$, appears to have little effect on the inferred σ_{bn}. A change of γ from 0 (flat distribution) to -2.0 (preponderance of low-mass components) results in the variation of σ_{bn} from 0.90 to 1.07 km/s.

Binary systems increase the errors in the determination of coordinates and proper motions by $0.1r^{-1}$ mas and $0.1r^{-1}$ mas/yr, respectively. Given that the median heliocentric distance of OB associations is $r = 1.7$ kpc the errors resulting from nonlinear motion of the photocenter are almost by an order of magnitude less than the threshold size of the error ellipsoid equal to 1.2 mas above which the five-parameter solution derived from Gaia data is rejected. Thus, the nonlinear motions of photocenters of binary systems do not cause a crucial increase of errors in determination of astrometric parameters.

We showed that the contribution of binary systems to the velocity dispersion inside OB associations ($\sigma_{bn} = 0.8-1.1$ km/s) is small compared to the velocity dispersion caused by turbulent motions inside giant molecular clouds, $\sigma_t = 4-5$ km/s.

The allowance for the effect of binary stars decreases the estimate of the velocity dispersion caused by turbulent motions. Its average value calculated for 28 OB associations decreases from 4.5 to 4.4 km/s, resulting in the increase of the median star-formation efficiency from 1.2 to 1.3% (for more details see [10]). The inferred low star-formation efficiency inside giant molecular clouds is consistent with other estimates [28−30].

REFERENCES

1. T. Prusti, J. H. J. de Bruijne, A. G. A. Brown, A. Vallenari, et al., Astron. Astrophys. **595**, A1 (2016).
2. A. G. A. Brown, A. Vallenari, T. Prusti, de J. H. J. Bruijne, et al., Astron. Astrophys. **616**, A1 (2018).

3. L. Lindegren, J. Hernandez, A. Bombrun, S. Klioner, et al., Astron. Astrophys. **616**, A2 (2018).

4. V. A. Ambartsumian, Astron. Zh. **26**, 3 (1949).

5. C. Blaha and R. M. Humphreys, Astron. J. **98**, 1598 (1989).

6. B. G. Elmegreen, Mon. Not. R. Astron. Soc. **203**, 1011 (1983).

7. R. B. Larson, Mon. Not. R. Astron. Soc. **194**, 809 (1981).

8. M. R. Krumholz, C. D. Matzner, and C. F. McKee, Astrophys. J. **653**, 361 (2006).

9. A. M. Melnik and A. K. Dambis, Mon. Not. R. Astron. Soc. **472**, 3887 (2017).

10. A. M. Melnik and A. K. Dambis, Mon. Not. R. Astron. Soc. **493**, 2339 (2020).

11. D. B. Sanders, N. Z. Scoville, and P. M. Solomon, Astrophys. J. **289**, 373 (1985).

12. B. D. Mason, D. R. Gies, W. I. Hartkopf, W. G. Bagnuolo, T. ten Brummelaar, and H. A. McAlister, Astron. J. **115**, 821 (1998).

13. H. Sana, in *The Lives and Death-Throes of Massive Stars,* Proc. IAU Symp. **329**, 110 (2017).

14. H. Sana, A. de Koter, S. E. de Mink, P. R. Dunstall, et al., Astron. Astrophys. **550**, A107 (2013).

15. M. Moe and R. di Stefano, Astrophys. J. Suppl. **230**, 15 (2017).

16. F. Arenou, X. Luri, C. Babusiaux, C. Fabricius, et al., Astron. Astrophys. **616**, A17 (2018).

17. C. Fabricius, U. Bastian, J. Portell, J. Castaneda, et al., Astron. Astrophys. **595**, A3 (2016).

18. N. Duric, *Advanced Astrophysics* (Cambridge Univ. Press, Cambridge, UK, 2004).

19. E. J. Aldoretta, S. M. Caballero-Nieves, D. R. Gies, E. P. Nelan, et al., Astron. J. **149**, 26 (2015).

20. E. Öpik, Publ. Observ. Astron. Univ. Tartu **28**, 1 (1924).

21. H. A. Abt, Ann. Rev. Astron. Astrophys. **21**, 343 (1983).

22. H. Sana and C. J. Evans, IAU Symp. **272**, 474 (2011).

23. D. Michalik, L. Lindegren, and D. Hobbs, Astron. Astrophys. **574**, A115 (2015).

24. H. A. Kobulnicky, D. C. Kiminki, M. J. Lundquist, J. Burke, et al., Astrophys. J. Suppl. **213**, 34 (2014).

25. O. Y. Malkov, V. S. Tamazian, J. A. Docobo, and D. A. Chulkov, Astron. Astrophys. **546**, A69 (2012).

26. G. N. Duboshin, *Celestial Mechanics: The Main Problems and the Methods* (Moscow, Nauka, 1975) [in Russian].

27. J. M. A. Danby, *Fundamentals of Celestial Mechanics,* 2nd ed. (Willmann-Bell, Richmond, VA, 1988).

28. P. C. Myers, T. M. Dame, P. Thaddeus, R. S. Cohen, R. F. Silverberg, E. Dwek, and M. G. Hauser, Astrophys. J. **301**, 398 (1986).

29. N. J. Evans, M. M. Dunham, J. K. Jorgensen, M. L. Enoch, et al., Astrophys. J. Suppl. **181**, 321 (2009).

30. P. Garcia, L. Bronfman, L.-A. Nyman, T. M. Dame, and A. Luna, Astrophys. J. Suppl. **212**, 2 (2014).

SPELL: OK